AFRL-RY-WP-TP-2008-1158

POST-CORRELATION SEMI-COHERENT INTEGRATION FOR HIGH-DYNAMIC AND WEAK GPS SIGNAL ACQUISITION (PREPRINT)

Chun Yang, Thao Nguyen, Erik Blasch, and Mikel Miller

Sigtem Technology, Inc.

JUNE 2008

AIR FORCE RESEARCH LABORATORY
SENSORS DIRECTORATE
WRIGHT-PATTERSON AIR FORCE BASE, OH 45433-7320
AIR FORCE MATERIEL COMMAND
UNITED STATES AIR FORCE

REPORT DOCUMENTATION PAGE

Form Approved
OMB No. 0704-0188

1. REPORT DATE *(DD-MM-YY)*	2. REPORT TYPE	3. DATES COVERED *(From - To)*
June 2008	Conference Paper Preprint	08 April 2005 – 08 May 2008

4. TITLE AND SUBTITLE
POST-CORRELATION SEMI-COHERENT INTEGRATION FOR HIGH-DYNAMIC AND WEAK GPS SIGNAL ACQUISITION (PREPRINT)

5a. CONTRACT NUMBER
FA8650-05-C-1828

5b. GRANT NUMBER

5c. PROGRAM ELEMENT NUMBER
65502F

6. AUTHOR(S)
Chun Yang (Sigtem Technology, Inc.)
Thao Nguyen and Mikel Miller (AFRL/RYRN)
Erik Blasch (AFRL/RYAA)

5d. PROJECT NUMBER
3005

5e. TASK NUMBER
13

5f. WORK UNIT NUMBER
300513CY

7. PERFORMING ORGANIZATION NAME(S) AND ADDRESS(ES)
Sigtem Technology, Inc.
1343 Parrott Drive
San Mateo, CA 94402-3630

Reference Systems Branch (AFRL/RYRN)
RF Sensor Technology Division
Assessment and Integration Branch (AFRL/RYAA)
Sensor ATR Technology Division
Air Force Research Laboratory, Sensors Directorate
Wright-Patterson Air Force Base, OH 45433-7320
Air Force Materiel Command, United States Air Force

8. PERFORMING ORGANIZATION REPORT NUMBER

9. SPONSORING/MONITORING AGENCY NAME(S) AND ADDRESS(ES)
Air Force Research Laboratory
Sensors Directorate
Wright-Patterson Air Force Base, OH 45433-7320
Air Force Materiel Command
United States Air Force

10. SPONSORING/MONITORING AGENCY ACRONYM(S)
AFRL/RYRN

11. SPONSORING/MONITORING AGENCY REPORT NUMBER(S)
AFRL-RY-WP-TP-2008-1158

12. DISTRIBUTION/AVAILABILITY STATEMENT
Approved for public release; distribution unlimited.

13. SUPPLEMENTARY NOTES
Paper produced under contract FA8650-05-C-1828 for technical report AFRL-RY-WP-TR-2008-1137, SOFTWARE TOOLKIT FOR NONLINEAR FILTERS FOR GLOBAL POSITIONING SYSTEM (GPS) OPERATIONAL CONTROL SEGMENT (OCS) ESTIMATION AND OTHER APPLICATIONS.

Conference paper published in the Proceedings of the ION-NTM/IEEE PLANS, Position Location and Navigation Symposium, 2008 (held in Monterey, CA, May 2008; Publisher: Institute of Electrical and Electronics Engineers Inc.).

PAO Case Number: RY 08-0202; Clearance date: 25 Jun 2008. The U.S. Government is joint author of this work and has the right to use, modify, reproduce, release, perform, display, or disclose the work. Paper contains color.

14. ABSTRACT
A new approach to weak GPS signal acquisition is presented in this paper. It belongs to the category of approaches that aim at enhancing the sensitivity of standalone GPS receivers without network assistance, which is also called unaided GPS receivers.

Acquisition and ultimate tracking of a weak GPS signal (e.g., in an in-door environment) faces several technical challenges, notably, possible data bit sign reversal every 20 ms and tolerable frequency error inversely proportional to the integration interval. Brute force search over all possible combinations of the unknown values is prohibitive computationally. Aided GPS relying on external infrastructure for timing, data bit, and frequency error information is costly. Coherent techniques such as the block accumulating coherent integration over extended interval (BACIX) have recently been proposed to extend coherent integration. *Abstract concludes on reverse side →*

15. SUBJECT TERMS

16. SECURITY CLASSIFICATION OF:			17. LIMITATION OF ABSTRACT:	18. NUMBER OF PAGES	19a. NAME OF RESPONSIBLE PERSON (Monitor)
a. REPORT	b. ABSTRACT	c. THIS PAGE			Thao Nguyen
Unclassified	Unclassified	Unclassified	SAR	16	19b. TELEPHONE NUMBER *(Include Area Code)* N/A

Standard Form 298 (Rev. 8-98)
Prescribed by ANSI Std. Z39-18

14. ABSTRACT (concluded)

Although efficient, such coherent methods may still be too expensive except for high-end receivers and may not maintain the SNR performance when there are large frequency changes over the intended integration interval.

In this paper, we set forth a novel method that utilizes the semi-coherent scheme for post-correlation integration, which is named as "block accumulating semi-coherent integration of correlations" or BASIC. It can be viewed as an extension of the BACIX algorithm. Although less sensitive than coherent integration, semi-coherent integration based on inter-block conjugate products is computationally more efficient. In addition, it can handle large frequency changes.

The BASIC algorithm is first formulated in the paper. Computer simulation results are then presented to illustrate operation and performance of the BASIC algorithm for joint estimation of the initial frequency, chirping rate (frequency rate), bit sync, and bit sign pattern.

Post-Correlation Semi-Coherent Integration For High-Dynamic and Weak GPS Signal Acquisition

Chun Yang
Sigtem Technology, Inc.
San Mateo, CA 94402

Thao Nguyen
Air Force Research Lab
WPAFB, OH 45433

Erik Blasch
Air Force Research Lab
WPAFB, OH 45433

Mikel Miller
Air Force Research Lab
WPAFB, OH 45433

***Abstract*–Acquisition and ultimate tracking of a weak GPS signal faces several technical challenges, notably, possible data bit sign reversal every 20 ms and tolerable frequency error inversely proportional to the integration interval. Brute force search over all possible combinations of the unknown values is computationally prohibitive. Assisted GPS relying on external infrastructure for timing, data bit, and frequency error information is costly. Coherent techniques such as the block accumulating coherent integration over extended interval (BACIX) have recently been proposed to increase coherent integration. Although efficient, such coherent methods may still be too expensive except for high-end receivers and may not maintain the SNR performance when there are large frequency changes over the extended integration interval.**

In this paper, we set forth a novel method that utilizes the semi-coherent scheme for post-correlation integration. It is named as block accumulating semi-coherent integration of correlations (BASIC) and can be viewed as an extension of the BACIX algorithm. Although less sensitive than coherent integration, semi-coherent integration based on inter-block conjugate products is computationally more efficient. In addition, it can handle large frequency changes.

The BASIC algorithm is first formulated in the paper. Computer simulation results are then presented to illustrate the operation and performance of the BASIC algorithm for joint estimation of the initial frequency, chirping rate (rate of change in frequency), bit sync, and bit sign pattern.

I. INTRODUCTION

A Global Positioning System (GPS) receiver needs to measure the distances to at least four GPS satellites at known orbital locations in order to obtain an estimate of its own position plus its clock error. These distances, also called pseudoranges, are obtained from the measured propagation delay times of the radio signals broadcast by the orbiting satellites to the GPS receiver, multiplied by the speed of light. The propagation delay time is measured as the difference between the time a particular event of the radio signal arrives at the receiver antenna and the time that same event leaves the satellite antenna. The time of arrival is tagged with the receiver clock, which may be biased and be subject to large clock drift, particularly in inexpensive commercial receivers. The time of transmission, as read from ultra-precise atomic clocks onboard GPS satellites, is encoded in the navigation message. Also modulated on the same radio signals are the ephemeris data which must be demodulated from the data bits to reconstruct the satellite orbital positions at the time of transmission [2, 3, 4, 5].

The received GPS signals must attain a minimum power level to ensure a GPS solution, which is routinely met when there is a clear line-of-sight (LOS) view from the receiver antenna to GPS satellites above the horizon. However, when the line-of-sight view between the receiver and a satellite is obstructed (e.g., due to foliage, mountains, buildings, or other structures) the GPS signal strength may be severely attenuated, leading to position fix with poor accuracy and even breakdown of tracking loops inside a regular receiver. It is therefore desired to improve GPS receiver sensitivity to operate on GPS signals of very low power level (or weak signals) to satisfy the requirements of location-based mobile e-commerce and emergency call location (E911).

One approach to acquiring weak GPS signals is assisted GPS (AGPS). The AGPS approach relies upon a wireless data link (or other means) to distribute, in real time, such information as time, frequency, navigation data bits, satellite ephemeredes, and approximate position as well as differential corrections to special GPS receivers equipped with a network modem so as to reduce the uncertainty search space, to help lock onto signals, and to assist navigation solution. This approach, however, comes with a heavy price associated with installing and maintaining the wireless aiding infrastructure and services required to provide the coverage.

To enable weak GPS signal acquisition, one known technique at the receiver end is to extend the signal integration time. Coherent integration is more gainful than the non-coherent counterpart [11]. However, when the coherent integration interval extends beyond, say, 20 ms, which is the duration of one data bit for GPS C/A-code, the sign reversal of navigation data bits becomes destructive if it occurs in the middle of a long coherent integration. As a result, an additional signal parameter, namely, the data bit transition, has to be searched in addition to the two usual parameters, code phase (time) and carrier frequency, beside the ID number of GPS satellites. This in fact constitutes a four dimensional search.

With nominally twenty-four active GPS satellites in orbit, the maximum number of visible satellites is about ten for a near-Earth receiver. For GPS C/A-code, the amount of search in time (code phase) is actually fixed. With a search step of a half code chip, there are 2046 steps needed to cover the entire code sequence of 1023 chips. Sequential stepping through all

the 2046 code phases, use of 2046 correlators in parallel, or a combination of sequential and parallel techniques are among a host of approaches of different complexity for code search and acquisition [2, 3, 4, 5].

However, the amount of search in frequency and in data bit transition increases as the coherent integration prolongs. The frequency uncertainty for a stationary user (due to the relative motion between the user and a GPS satellite and the receiver local clock drift) is typically ±5 kHz. When the integration time is increased from the C/A-code epoch of 1 ms to, say, 20 ms, the amount of frequency search needs to be increased by 20-fold. Similarly, the number of possible locations of data bit transition also increases as the coherent integration interval increases. The number of possible combinations increases exponentially. There are also second-order effects associated with the extended coherent integration. This mainly involves changes in the carrier frequency and code chipping rate due to acceleration and instability of local clock, which may become significant over long integration intervals.

A typical search process for a GPS receiver employing 1 ms correlation for the C/A-code using either sequential or parallel correlators involves search in four dimensions. The first search is to look for a visible GPS satellite among those active satellites in orbit. For a given satellite, parametric search is conducted in three nested loops. The outer parametric loop is typically the frequency search, which steps through the frequency uncertainty interval 500 Hz per step. The selected frequency offset (a frequency bin) is added to the nominal frequency to control the carrier numerically controlled oscillator (NCO) whose output drives the in-phase and quadrature components of the reference carrier for down-conversation to baseband.

The middle parametric loop is the code phase search over the entire code epoch of 1023 chips, a half chip per step (a code lag) typically. In a correlator-based receiver, the code phase search may be done sequentially one code phase at a time or in parallel with all code phases searched at the same time.

The inner loop accumulates the 1 ms correlations for each search grid point in terms of a frequency bin and a code lag over a certain period of time (a dwell time), during which the signal is added up for detection. Under normal signal strength, the dwell time is usually chosen to be several ms wherein the 1 ms correlations are power-combined (i.e., the non-coherent integration) with the navigation data bit transitions squared out, thus not being an issue. However, for weak GPS signals, the dwell time may extend beyond 20 ms for coherent integration where the navigation data bit transition plays a critical role.

When the despreading correlation is carried out every 1 millisecond, the complex correlation is available at the rate of 1 kHz. To further integrate, there will be twenty 1 millisecond correlations (20 data points) per a data bit. When coherent integration is beyond two data bits, the number of possible bit transitions is large and bit transition patterns become complicated. There are, consequently, outstanding problems with known techniques for weak GPS signal acquisition and tracking in a standalone high-sensitivity receivers.

Recently, a new approach for weak GPS signal acquisition without network assistance was presented in [10], which belongs to the category of approaches aimed at enhancing the sensitivity of standalone GPS receivers (or unaided GPS receivers). The approach, named the "block accumulating coherent integration over extended interval – BACIX" is based on three ideas. The first idea of successive sign reversal of 1 ms correlations per block (*i.e.*, 20 ms) enables data bit transition detection and data bit sign correction within a data bit interval. This is in sharp contrast to conventional methods that only process half blocks at a time (undesired SNR loss) or are stretched over two blocks (excessive latency). In addition, it allows for efficient use of Fast Fourier Transform (FFT), which only needs to be calculated once and manipulated simply for all tentative bit alignments. As the second idea, the FFT is implemented as a bank of bandpass filters to integrate blocks of correlations in a coherent manner, as opposed to conventional phase rotation that can only handle one bandpass filter at a time and requires excessive frequency search. Finally, the third idea optimizes the overall computation by pruning unlikely branches of the search paths in partial sums. Such a block accumulating coherent integration boosts the signal power while reducing noise despite unknown data bit transitions and other variations that may occur during the extended coherent integration intervals.

Another new method for weak GPS signal acquisition without network assistance was presented in [12], which is particularly suitable for high dynamic applications. In the method, the post-correlation signal is modeled as a chirp or linear frequency modulated (LFM) signal wherein the effect of high dynamics is accounted for by the chirping rate, albeit unknown. The Wigner-Ville distribution (WVD) is used to represent the signal energy in the time-frequency plane while the Hough transform (HT) integrates the energy belonging to a chirp signal, which distributes along a line in the time-frequency plane [1]. Similarly, the Radon transform can be used in place of the Hough transform to integrate the chirp energy along a line in the time-frequency plane [7]. However, the combination of the WVD and HT, the Wigner-Hough transform (WHT), or the combination of the WVD and RT, the Wigner-Radon transform (WRT), cannot be applied directly to the despread correlations because of the presence of unknown data bits. The new method is a block-implemented WHT/WRT using the intra-block conjugates products [12]. They were shown to be able to jointly estimate the initial frequency, chirping rate (frequency rate), and bit sync but not the bit sign pattern.

In this paper, a novel approach for weak GPS signal acquisition without network assistance is set forth. The approach is named the "block accumulating semi-coherent integration of correlations – BASIC," which can be viewed as an extension of the BACIX algorithm in two aspects. First, it can handle large frequency changes. Second, it is

computationally more efficient. The novel BASIC algorithm is based on the semi-coherent integration scheme as analyzed in [11] and makes use of block conjugate products [12].

After introducing a complex model for post-correlation GPS signals in Section II, we describe the BASIC algorithm using the inter-block conjugate products in Sections III. In Section IV, simulation results are presented to illustrate the operation and performance of the BASIC algorithm for joint estimation of the initial frequency, chirping rate (frequency rate), bit sync, and bit sign pattern. A summary is provided in Section V with concluding remarks and future work.

II. COMPLEX MODEL FOR POST-CORRELATION GPS SIGNALS

Consider a scheme for acquiring GPS signals via search in time and frequency. Assume that the frequency search step is 500 Hz, the code search step is half a chip, and the integration interval of the despreading correlation is 1 ms. Such integration can tolerate ±250 Hz errors in frequency and ±¼ chips. For a search grid, the worst code uncertainty is a quarter of a chip duration ($\Delta t = T_c/4$) and the worst Doppler uncertainty is Δf = 250 Hz. As a result, the maximum loss in a 1 millisecond coherent integration (T_i = 1 millisecond) is

$$\begin{aligned}\text{Loss} &= 20\log_{10}R(\Delta t) + 20\log_{10}[\sin(\pi\Delta f T_i)/\pi\Delta f T_i] \\ &= 20\log_{10}(0.75) + 20\log_{10}(0.9) = -3.4 \text{ dB}\end{aligned} \quad (1)$$

where $R(\cdot)$ stands for the correlation function with an ideally triangular shape.

The resulting complex correlation is unique for each GPS satellite and can be written as:

$$x_n = b_n A_n \exp\{j[2\pi(f_0 n T_s + \alpha n^2 T_s^2) + \phi_0]\} + w_n \quad (2)$$

where x_n is the complex post-correlation signal with the sample index n, A_n is the amplitude, ϕ_n is the initial phase, T_s = 1 ms is the integration interval with the sampling rate of 1 kHz, b_n = ±1 is the unknown data bit, f_0 is the initial frequency, α is the chirping rate (sometimes $\alpha/2$), and w_n is an uncorrelated noise with zero mean and unity variance.

For GPS C/A-codes, the baud rate is 50 Hz and each data bit thus has a periodicity of 20 ms. There will be 20 samples per data bit of the same sign, but it may change sign from one data bit to the next. Knowing which sample is the start of a data bit is called the bit sync. Without knowing the bit sync, a perfect correction may be destroyed if there is a data bit sign reversal in the middle of integration. It is equally important to determine the sign of data bits, from which the navigation messages can be demodulated.

The instantaneous frequency in (2) represents the frequency error between the incoming signal and the local carrier replica, which can be written as:

$$\Delta f_n = f_0 n T_s + \alpha n^2 T_s^2 \quad (3)$$

For the local carrier replica fixed at a search frequency, the complex model in (2) is useful as long as the frequency error, albeit being time-varying, remains within ±250 Hz. Otherwise, the search switches to another search frequency. Over a time interval of T_i, the maximum chirp rate for a fixed carrier replica is:

$$\alpha = -sign(f_0)\frac{500 - |f_0|}{T_i} \quad (4)$$

where $sign(\cdot)$ is a sign function, so that the change in frequency is less than 500 Hz in one second. The maximum chirp rate is therefore α = 500 Hz/s. At L1 = 1575.42 MHz, the frequency change over one second is related to the underlying acceleration (in g = 9.8 m/s^2) by the factor of 51.49 Hz/g/s.

The signal amplitude A_n includes a factor $R(\Delta\tau)$ related to timing error $\Delta\tau$ and a factor $\sin(\pi T_s \Delta f)/\pi T_s \Delta f$ related to frequency error Δf [2, 3, 4, 5]. As a result, the signal amplitude A_n is also subject to variations due to changes in Δf. Since the change is rather small, the amplitude is assumed to be constant for simplicity in this paper.

For weak signal acquisition and other applications, it is desired to further integrate the 1 ms correlations, x_n, over a rather long period of time, T_i. Because of the unknown data bits b_n and varying frequency errors Δf, it is counter-productive to sum complex correlations x_n directly. Squaring can move both the data bit and the unknown frequency error and allows for direct summation. However, this non-coherent integration also squares noise [11] and further strips off all valuable information about the signal that is needed for subsequent processing in a GPS receiver. In contrast, a semi-coherent integration scheme is used to implement the BASIC algorithm based on inter-block conjugate products as described below.

III. BASIC WITH INTER-BLOCK CONJUGATE PRODUCTS

Referring to Fig. 2, consider two consecutive blocks denoted by:

$$\underline{y}_k = [x_{ki}, \quad i = 1,...,M] = [x(t) \quad t = (M(k-1)+i)T_s] \quad (5a)$$

$$\underline{y}_{k+1} = [x_{(k+1)i}, \quad i = 1,...,M] = [x(t+\tau), \quad t = (M(k-1)+i)T_s] \quad (5b)$$

where k = 1, …, K-1 is the block index, $\tau = MT_s$ = 20 ms is the fixed delay between two blocks with for M = 20 and T_s = 1 ms.

Construct a (K-1)×M matrix of inter-block conjugate products as:

$$\begin{aligned}Z &= [z_{ki}, \quad i = 1,..., M, \quad k = 1,..., K-1] \\ &= [z(t), \quad t = (20(k-1)+i)T_s]\end{aligned} \quad (6a)$$

$$z_{ki} = x_{(k+1)i}x_{ki}^*, \; i = 1, \ldots, M, \; k = 1, \ldots, K\text{-}1 \quad (6b)$$

$$z(t) = x(t+\tau)x^*(t), \quad t = (M(k\text{-}1)T_s, \; i = 1, \ldots, M, \; k = 1, \ldots, K\text{-}1 \quad (6c)$$

With the chirp signal modeled in (2), an inter-block conjugate product of (6) can be further written as:

$$z(t) = x(t+\tau)x^*(t) = b(t)b(t+\tau)A^2 e^{j2\pi(f_0\tau+\alpha\tau^2+2\alpha\pi t)} \quad (7a)$$

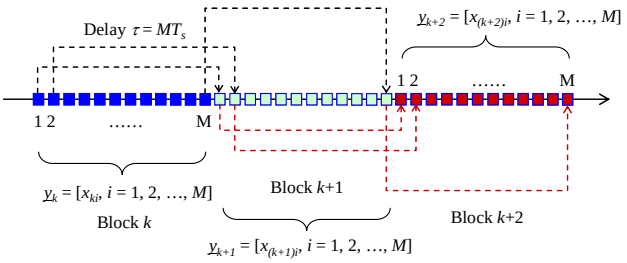

Fig. 1. Time Diagram for Inter-Block Conjugate Products

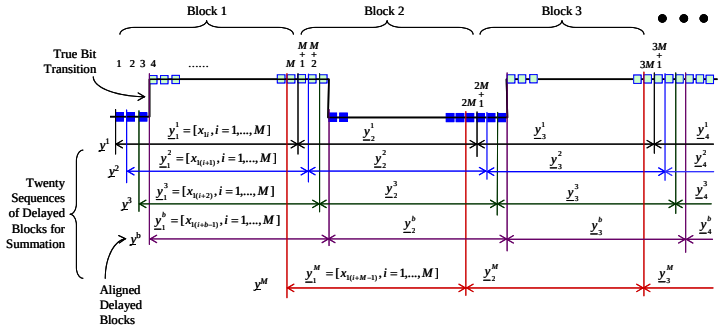

Fig. 2. Twenty Delayed Sums for Bit Sync

$$z_{ki} = x_{(k+1)i} x_{ki}^* = b_k b_{k+1} A^2 e^{j2\pi(f_0\tau + \alpha\tau^2 + 2\alpha M T_s^2[M(k-1)+i])} \tag{7b}$$

The complex exponential in (7) does not contain any t^2 term, which is eliminated by the delayed conjugate products. Putting aside the unknown sign of data bit products $b_k b_{k+1}$, the application of FFT on z_{ki} over k will produce a peak at $2\alpha\tau$ for each i, from which the chirp rate can be estimated. The complex peaks can be FFT-analyzed again over i to further strengthen the signal. This in fact involves a 2D FFT [6, 9].

Another way to strengthen the signal is to sum up all the terms pertaining to a block k (*i.e.*, straight summation over i for each k). This will incur a small loss but reduce computation as compared to the use of FFT. The averaged term can be written as:

$$\bar{z}_k = \sum_{i=1}^{M} z_{ki} = b_k b_{k+1} A^2 \frac{\sin(2\pi\alpha M^2 T_s^2)}{\sin(2\pi\alpha M T_s^2)} \times e^{j2\pi\alpha(M+1)T_s^2} e^{j2\pi(f_0\tau + \alpha\tau^2 + 2\alpha T_s^2 M^2(k-1))} \tag{8a}$$

$$\approx b_k b_{k+1} M A^2 e^{j2\pi(f_0\tau + \alpha\tau^2 + 2\alpha T_s^2 M^2(k-1))} \tag{8b}$$

Then applying the FFT to $\bar{z}_k$ over k, without considering the data bits, produces:

$$Z_v = \mathcal{F}_k\{[(\bar{z}_k,\quad k = 1,2,\ldots,K),\quad \underline{0}_{\kappa(K-1)}]\} \tag{9}$$

where κ is the factor of K-1 zeros padded to $\bar{z}_k$ prior to the FFT.

The peak location of Z_v within $\pm(\kappa+1)K/2$ is obtained as:

$$\hat{l} = \arg\max_v |Z_v| \tag{10}$$

The peak location $\hat{l}$ provides an estimate of the quantity $2\alpha\tau$, from which the chirping rate α can be estimated directly as:

$$\hat{\alpha}(\tau) = \frac{1}{2} \frac{\hat{l}}{T_s^2 M^2 (K-1)(\kappa+1)} \tag{11}$$

Different from the intra-block conjugate products where the product of two samples within a block aligned to the same data bit is always 1 [12], the inter-block conjugate products, however, may have different signs. This therefore requires determination of data bit signs in addition to the location of data bit transitions (bit sync). One simple approach to bit sync is to maintain twenty sums of blocks. The start of blocks of a sum corresponds to a possible bit transition location within 20 ms and the block in one sum is delayed by one sample (1 ms) relative to the preceding sum as shown in Fig. 2.

The k^{th} block in the b^{th} sum is therefore constructed as:

$$\underline{y}_k^b = [x_{20(k-1)+i+b-1},\quad i = 1,\ldots,20] = [x_{k(i+b)},\quad i = 1,\ldots,M],$$
$$b = 1, \ldots, 20,\ k = 1, \ldots, K \tag{12}$$

The averaging in (8) is applied to each and every block of the twenty partial sums. These averaged blocks are then accumulated with bit signs rectified using the method described below. At this point, denote the twenty sums over K blocks by $S^b(\underline{y}_k^b,\ n = 1, \ldots, K)$. The partial sum that produces the maximum value provides an estimate of the data bit transition (*i.e.*, the tentative bit sync) as:

$$\hat{b} = \arg\max_b S^b(\underline{y}_1^b, \ldots, \underline{y}_n^b, \ldots, \underline{y}_K^b) \tag{13}$$

The method to determine data bit signs and accumulate the partial sums with bit signs rectified is now presented. For the aligned sum, *i.e.*, the particular sum among the twenty delayed sums that happens to have the start and end of its blocks coincide with data bits, the average signal model in (8) is repeated below with simplified notations as:

$$\bar{z}_k = \delta_k B e^{j(2\pi\gamma k + \phi_0)} \tag{14}$$

where $\delta_k = b_k b_{k+1}$, $B = MA^2$, $\gamma = 2\alpha T_s^2 M^2$, $\phi_0 = 2\pi(f_0\tau + \alpha\tau^2 - 2\alpha T_s^2 M^2)$. It is interesting to note that for non-aligned delayed sums, δ_k is no longer binary-valued because of possible sum of samples across sign reversal.

We therefore start with a sequence of samples $\bar{z}_k$, k = 1, 2, …, K-1, available at 50 Hz. Each sample interval is the same as a data bit of 20 ms. To determine the sign for each sample δ_k while estimating the unknown frequency γ, we conduct four steps. The first step consists of pre and post zero-padding each sample so as to maintain its timing order in the original sequence:

$$\underline{h}_k = [\underline{0}_{k-1}^T \quad \bar{z}_k^T \quad \underline{0}_{K-k-1}^T]^T,\ k = 1, 2, \ldots, K\text{-}1 \tag{15}$$

The second step is to apply the FFT to the K-1 vector $\underline{h}_k$ expanded from a single sample $\bar{z}_k$ as:

$$H_k(l) = \mathcal{F}\{\underline{h}_k\},\ l = 1, 2, \ldots, K\text{-}1 \tag{16}$$

where l is the index of the frequency bin with a resolution inversely proportional to the data length $(K\text{-}1)MT_s$ (zero-padding is again possible if a refined size of the frequency bin is desired).

The third step is to obtain the twenty partial sums up to k while estimating the sign δ_k. Assume that we already have estimated the bit signs up to k-1 for the b^{th} partial sum, denoted by $B_{k-1}^b(l)$, and obtained the corresponding partial sums up to k-1, denoted by $S_{k-1}^b(l)$, for l = 1, 2, …, K-1 and b = 1, 2, …, M. Then, the partial sums and bit pattern up to k are obtained by:

$$S_k^b(l) = S_{k-1}^b(l) + \hat{\delta}_k^b(l) H_k^b(l) \tag{17a}$$

$$B_k^b(l) = [B_{k-1}^b(l), \quad \hat{\delta}_k^b(l)] \tag{17b}$$

$$\hat{\delta}_k^b(l) = \arg \max_{\delta \in [-1,1]} |\, S_{k-1}^b(l) + \delta_k^b H_k^b(l) \,|,$$
$$l = 1, 2, \ldots, K\text{-}1 \text{ and } b = 1, 2, \ldots, M \tag{17c}$$

In the fourth step, the maximum partial sum across the frequency bins for each tentative bit transition is first obtained as:

$$\hat{l}^b = \arg \max_{l \in [1,\ldots,K-1]} |\, S_{K-1}^b(l) \,|,\ b = 1, 2, \ldots, M \tag{18}$$

Then, the maximum partial sum across all tentative bit transitions is obtained as:

$$\hat{b} = \arg \max_{b \in [1,\ldots,M]} |\, S_{K-1}^b(\hat{l}^b) \,| \tag{19}$$

which provides the best estimate of data bit transition, thus achieving the bit sync. Finally, the best frequency bin for the maximum partial sum at the estimated bit sync is given by:

$$\hat{l} = \hat{l}^{\hat{b}} \tag{20}$$

and the corresponding chirping rate α can be estimated directly from (11).

The total number of possible sequences to maintain is $M(K\text{-}1)$ in the above computation. However, it is possible to trim down the number of possible bit sequences in frequency bins and/or bit transitions after few samples are integrated by discarding the smallest partial sums, thus saving computation and memory.

Unique to the inter-block conjugate products is the fact that the sign sequence as determined above is a differential bit sequence $\{\delta_k = b_k b_{k+1}\}$. The original bit sequence $\{b_k\}$ has to be reconstructed from it. To illustrate, consider the example listed in Table 1. The first row in Table 1 shows the original bit sequence b_k = {1, -1, -1, 1, -1, 1, 1, …}. The second row is the differential bit sequence is $b_k b_{k+1}$ = {-1, 1, -1, -1, -1, 1, …}.

The inter-block conjugate products allow for the estimation of the differential bit sequence δ_k using (17) from the average samples $\bar{z}_k$. However, for the very first sample $\bar{z}_1$, we have the initial conditions $S_0^b(l) = 0$. δ_1 could be either 1 or -1. If the first selected sign matches the true differential bit, the remaining signs will reproduce the underlying differential bit sequence exactly. Otherwise, it will differ as being the complement.

For the data listed in Table 1, the first sign for the estimated differential bit is fixed at 1, which is the bolded number in the third row of Table 1. Since it differs from the first true sign, the estimated differential bits (third row) are complementary of the true differential bits (second row). Taking complement of the estimated differential bit sequence (called the negative logic) in the fourth row turns out to be the same as the true differential bits (second row).

When reconstructing the initial bit sequence from the estimated differential bit sequence, one also needs to select the sign for the very first bit. Using the positive and negative logic with the first bit fixed as "1", the reconstructed bit sequences are shown in the fifth and sixth rows of Table 1, respectively. Clearly, the sequence with negative logic is correct (the sixth row vs. first row) for the example shown in Table 1. This ambiguity in the bit sequence reconstruction can be easily solved by applying them back to the data samples and the correct one will result in the same sign for all samples and the resulting sum is bigger.

For the signal model in (14), the sign-rectified sum $S_{K-1}^{\hat{b}}(\hat{l})$ may exhibit two peaks of equal magnitude at frequency bins, say, $\hat{l}_1$ and $\hat{l}_2$ for two differential bit sequences $B_{K-1}^{\hat{b}}(\hat{l}_1)$ and $B_{K-1}^{\hat{b}}(\hat{l}_2)$, respectively. When applied to the samples $\bar{z}_k$, the correct differential bit sequence will render the signs all 1's or -1's whereas the incorrect sequence makes it +1 and -1 alternatively. Assume that $\hat{l}_1$ corresponds to the correct peak, which is given by $\hat{\delta}(\hat{l}_1) exp\{j2\pi\hat{l}_1 k\} = exp\{j2\pi\hat{l}_1 k\}$ because $B_{K-1}^{\hat{b}}(\hat{l}_1) = \{\hat{\delta}(\hat{l}_1) = 1$ or -1 for all $k\}$. It can be shown that the second peak location is related to the correct peak location by $\hat{l}_2 = \hat{l}_1 \pm ½$ in units of normalized frequency. Then, the peak value can be evaluated as:

$$exp\{j2\pi\hat{l}_2 k\} = exp\{j2\pi(\hat{l}_1 \pm ½)k\}$$
$$= exp\{j2\pi\hat{l}_1 k\} exp\{\pm j\pi k\} = (\pm 1)^{k+1} exp\{j2\pi\hat{l}_1 k\} \tag{21}$$

The sign term of (21) is cancelled out by the estimated differential bit $B_{K-1}^{\hat{b}}(\hat{l}_2) = \pm 1$, leading to the same value as the correct peak. Although the false peak parameters are correctly estimated, they can be distinguished from the true signal parameters by FFT-analyzing the de-chirped de-modulated signal samples, from which the initial frequency can be estimated as:

Table 1. Reconstruction from Differential Bit Sequence

Initial Bit Sequence:	b_k	1	-1	-1	1	-1	1	1	…
Differential Sequence:	$b_k\, b_{k+1}$	/	-1	1	-1	-1	-1	1	…
Estimated Differential:	δ_k	/	**1**	-1	1	1	1	-1	…
Complementary (Negative)	$\bar{\delta}_k$	/	-1	1	-1	-1	-1	1	…
Reconstructed (Positive):	$\hat{b}_k^{Pos}$	**1**	1	-1	-1	-1	-1	1	…
Reconstructed (Negative):	$\hat{b}_k^{Neg}$	**1**	-1	-1	1	-1	1	1	…

Table 2. Bit Sign Determination

k	1	2	3	4	5	6	7	8	9	10	11	12	13	14	15	16	17	18	19	20
b_k	**-1**	**1**	**1**	**-1**	**1**	**-1**	**-1**	**-1**	**1**	**-1**	**1**	**1**	**1**	**1**	**-1**	**-1**	**1**	**-1**	**1**	**1**
δ_k	/	-1	1	-1	-1	-1	1	1	-1	-1	-1	1	1	1	-1	1	-1	-1	-1	1
$\hat{\delta}_k^1$	/	1	-1	1	1	1	-1	-1	1	1	1	-1	-1	-1	1	-1	1	1	1	-1
$\delta_k\hat{\delta}_k^1$	/	-1	-1	-1	-1	-1	-1	-1	-1	-1	-1	-1	-1	-1	-1	-1	-1	-1	-1	-1
$\hat{b}_k^{1p}$	1	1	-1	-1	-1	-1	1	-1	-1	-1	-1	1	-1	1	1	-1	-1	-1	-1	1
$\hat{b}_k^{1n}$	**1**	**-1**	**-1**	**1**	**-1**	**1**	**1**	**1**	**-1**	**1**	**-1**	**-1**	**-1**	**-1**	**1**	**1**	**-1**	**1**	**-1**	**-1**
$\hat{\delta}_k^2$	/	1	1	1	-1	1	1	-1	-1	1	-1	-1	1	-1	-1	-1	-1	1	-1	-1
$\delta_k\hat{\delta}_k^2$	/	-1	1	-1	1	-1	1	-1	1	-1	1	-1	1	-1	1	-1	1	-1	1	-1
$\hat{b}_k^{2p}$	1	1	1	1	-1	-1	-1	1	-1	-1	1	-1	-1	1	-1	1	-1	-1	1	-1
$\hat{b}_k^{2n}$	1	-1	1	-1	-1	1	-1	-1	-1	1	1	1	-1	-1	-1	-1	-1	1	1	1

$$(\hat{f}_0, \hat{\alpha}, \hat{b}) = \arg\max_{\iota_i, i} \max_{f_0} |\, FFT\{\left[b_n^{\iota_i} \exp(-j2\pi \iota_i n) x_n, \quad n = 1,..., N\right]\}|,$$
$$\iota_i = 1, 2 \text{ and } i = 1, 2 \qquad (22)$$

The maximization of (22) provides the global peak location indices among the search variables i, ι_i, and the FFT frequency bin f_0. The frequency bin index of the FFT is then translated into the initial frequency estimate $\hat{f}_0$, the index i is translated in to the chirping rate $\hat{\alpha}$ via $\hat{l}$, and the logic index ι_i is translated into the estimated bit sequence $\hat{b}$.

Clearly, a much simpler algorithm results if the signal is of low dynamics, *i.e.*, $\alpha \approx 0$ Hz/s^2. The application of FFT over the pre and post zero-padded samples as in (16) is no longer necessary. This will considerably save computation time. The bit sign selection remains the same as in (17) except it is now only applied to one sequence (*i.e.*, $l = 0$). There will be no ambiguity due to double peaks but one still needs to distinguish between the positive and negative logic used in reconstructing the bit sequence from the estimated differential bit sequence. This can be easily done by picking up the one that has a bigger peak in the FFT applied to the corresponding bit-wiped samples.

Between the two extremes (*i.e.*, the full search with FFT in (16) and $l = 0$ for $\alpha \approx 0$ as described above), it is possible to consider a small number of chirping rates to account for medium dynamics.

In summary, the post-correlation integration involves search in data bit transition, data bit sign, initial frequency, and chirping rate. Several approximation techniques are presented to reduce computation. The inter-block conjugate products transform the simultaneous search in the initial frequency and chirping rate into two one-dimensional searches in sequence. Binary bit sign search is done with pruning to limit the tree growth. These and other features make the BASIC algorithm computationally viable as shown in the simulation examples below.

IV. SIMULATION RESULTS AND ANALYSIS

Simulation examples are presented below to illustrate the operation and performance of the method using inter-block conjugate products for joint estimation of signal parameter estimation and bit pattern as well as bit sync. In the first simulation example, we also consider an ideal case where there is no noise and no data modulation. The integration interval is again 1 s with $N = 1000$ for $T_s = 1$ ms. The data are divided into $K = 50$ blocks, each with $M = 20$ samples. The initial phase is $\theta = 32^o$, the initial frequency is $f_0 = -250$ Hz, and the chirping rate is $\alpha/2 = 250$ Hz/s.

Fig. 3 shows the 2D FFT applied to the inter-block conjugate products Z as defined in (20). The peak value is 948.23 vs. the full value of 20×49 = 980 and the peak location along k provides an estimate of the chirping rate, which is 245 Hz/s without interpolation vs. the true value of $\alpha/2 = 250$ Hz/s. The apparent errors in the peak value and chirping rate are due to quantization error. Either zero-padding prior to taking FFT or curve-fitting around the peak can reduce such quantization errors.

Fig. 4 shows the FFT applied to the average samples $\bar{z}_k$ with $\kappa = 7$ as in (9). The FFT length is therefore $(\kappa+1)\times K = 8\times 49 = 392$. The peak value is 963 vs. the full value of 980 and the peak location provides an estimate of the chirping

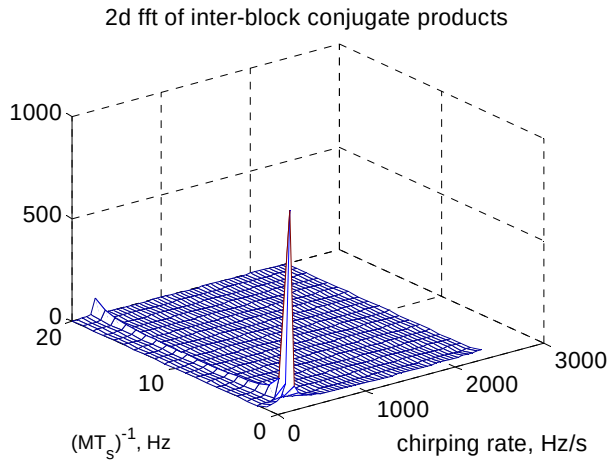

Fig. 3. 2D FFT Applied to *Z*

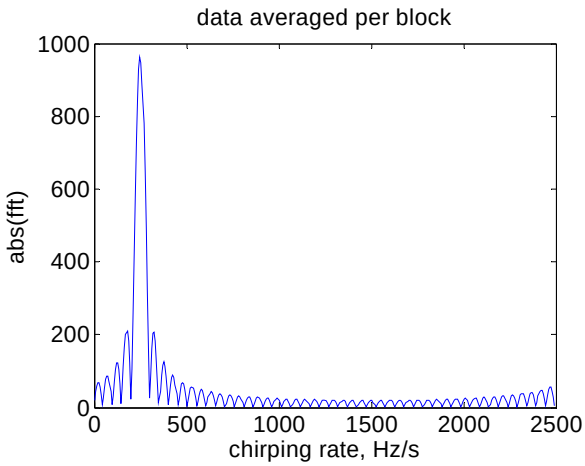

Fig. 4. FFT Applied to Samples Averaged per Block

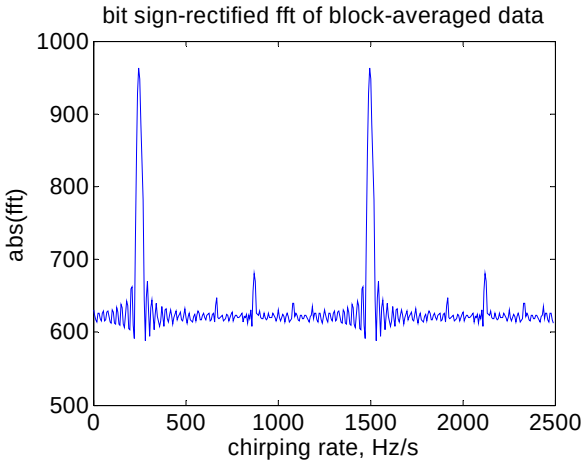

Fig. 5. FFT Applied to Bit Sign-Rectified Samples Averaged per Block During Search

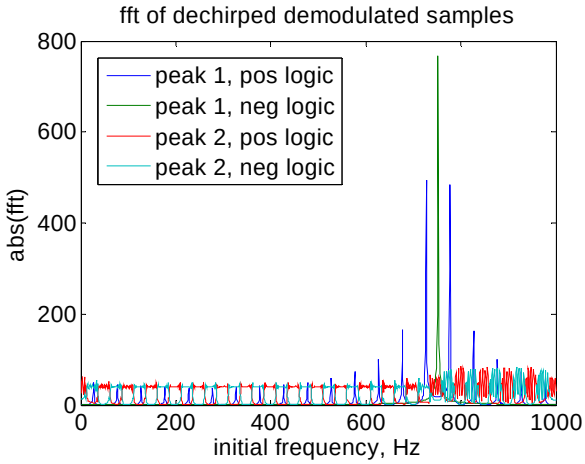

Fig. 6. FFT of Dechirped and Demodulated Samples

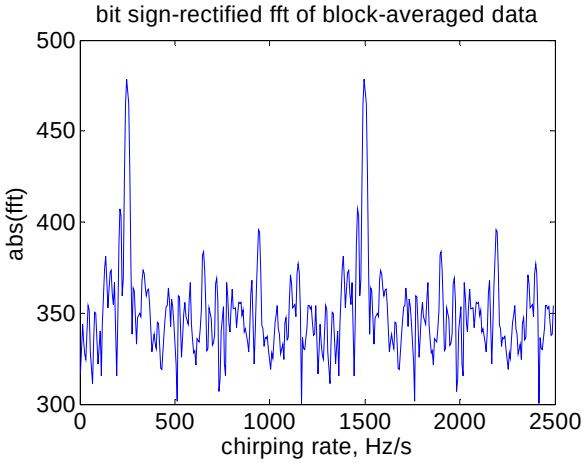

Fig. 7. FFT Applied to Bit Sign-Rectified Samples Averaged per Block During Search for SNR = -3 dB

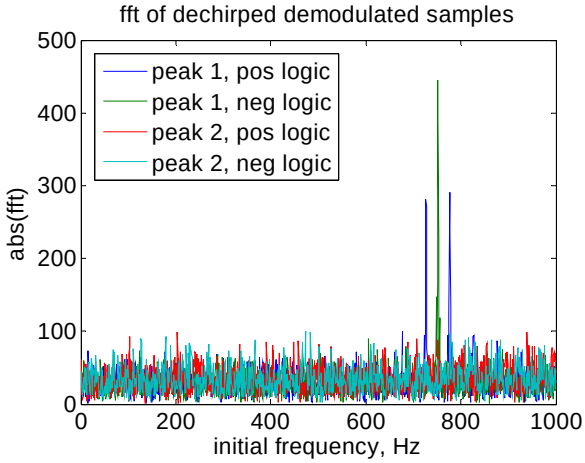

Fig. 8. FFT of Dechirped and Demodulated Samples For SNR = -3 dB

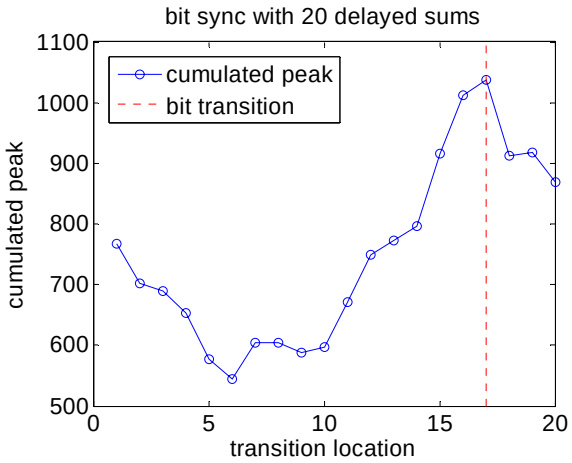

Fig. 9. Cumulative Peaks for Bit Sync (3 s)

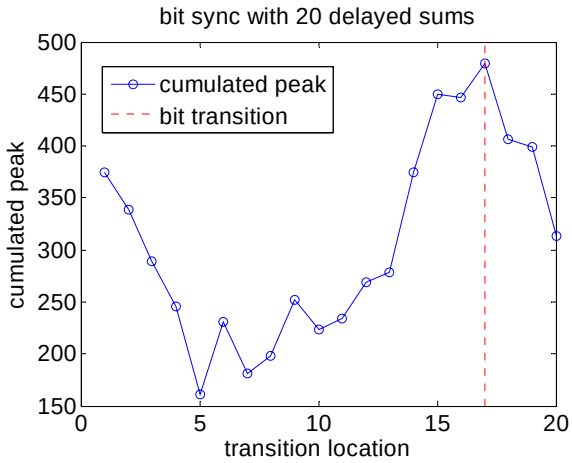

Fig. 10. Cumulative Peaks for Bit Sync for SNR = -3 dB (1 s)

rate according to (11), which is 248.725 Hz/s vs. the true value of α = 250 Hz/s. As indicated by (8), the *sinc* function is clearly visible from Fig. 4, which introduces a loss to the peak value and sidelobes. The latter may be attenuated to some extent when a windowing function is used.

In the second simulation example, all the conditions are kept same as in the first simulation except data bits are now modulated on to the samples. In the example, the first bit transition occurs between the 16th and 17th samples. In other words, the 16th sample is the end of the first incomplete data bit while the 17th sample is the start of a second data bit.

For the partial sum that has the correct alignment, Fig. 5 shows the bit sign-rectified FFT of the block-averaged samples, obtained using (17). The length of FFT is $(\kappa+1)\times K$ = 392 for κ = 7. As analyzed above, there are two peaks of equal strength of 963 at $\hat{\alpha}_1$ = 248.73 Hz/s and $\hat{\alpha}_2$ = -994.90 Hz/s, respectively, which are separated by a half of the *x*-axis scale in Fig. 5, which is 1250 Hz/s.

For each peak, there is an associated pattern of differential bits determined with the first sign fixed at 1. As explained in Table 1or each differential bit pattern, two possible bit sequences are reconstructed using a positive logic and a negative logic, respectively. Table 2 summarizes the results. The first row lists the first 20 signs of the original bit sequence. The second row shows the corresponding differential bit sequence. The next three rows list the estimated differential bit sequence associated with the first peak of Fig. 5 with the first sign fixed at 1 (3rd row), the reconstructed bit sequence using the positive logic (4th row), and the reconstructed bit sequence using the negative logic (5th row). The last three rows list the estimated differential bit sequence associated with the second peak of Fig. 5 with the first sign fixed at 1 (6th row), the reconstructed bit sequence using the positive logic (7th row), and the reconstructed bit sequence using the negative logic (8th row).

To test which one of these four possibilities is true, the original signal samples are dechirped with the estimated chirping rate $\hat{\alpha}_1$ and $\hat{\alpha}_2$ and demodulated with the bit sequences. The FFT is then applied to the dechirped and demodulated samples with the results shown in Fig. 6. Clearly, the negative logic bit sequence associated with the first peak (6th row in Table 2) is the correct estimate (except for a complementary sign difference). The peak location at frequency bin 751 provides an estimate of the initial frequency as (751-1000) = -249 Hz vs. the true value of f_0 = -250 Hz. The false peaks have 50 Hz harmonics reflecting the underlying data bits. In the third simulation example, all the conditions are kept same as in the second simulation with complex noise added such that the resulting SNR is -3 dB. Under the Nyquist rate, the signal passes through a low pass filter with an equivalent bandwidth of $\pm f_s/2$. For T_s = 0.001 s, SNR = -3 dB results from A = 0.7, which also corresponds to C/N_0 = 27 dB-Hz.

Again, for the partial sum that has the correct alignment, Fig. 7 shows the bit sign-rectified FFT of the block-averaged samples. Fig. 8 shows the FFT of dechirped and demodulated samples. Compared to Figs. 5 and 6, Figs. 7 and 8 show signal peaks lowered by a factor of two, consistent with SNR = -3 dB. However, the peaks remain at the same locations, thus providing the correct estimates of chirping rate, initial frequency, bit pattern, and bit sync.

Fig. 9 shows the twenty delayed sums for the case without noise over an interval of 3 s. The peak is around the correct bit transition location and the valley is about 10 samples away from the peak (partial sums starting around the middle of a data bit). However, the peak is not as sharp as the method using the intra-block conjugate products [12]. This may be due to the fact that complex exponentials across a block (vs. within a block) prevent samples that have opposite signs from complete cancellation. The flattened peak makes precise bit sync difficult over a short data span.

Fig. 10 shows the twenty delayed sums for SNR = -3 dB over a 1 s interval. The cumulated peak corresponds to the true bit transition, thus achieving bit sync. However, we observed cases where the peak location is with two samples (±2 ms) of the true bit transition. To note, in practical systems, it may take thousands of bits (in seconds to minutes)

to firmly establish bit sync, followed by continuous monitoring of bit transitions and bit re-sync if necessary.

V. CONCLUSIONS

In this paper, the GPS signal after the 1 ms despreading integration was modeled as a modulated chirp signal where in the binary modulation represents the data bits of navigation message while the chirp accounts for changes in residual Doppler frequency.

To further integrate the signal over a rather long period of time, the semi-coherent integration scheme (BASIC) was used on the inter-block conjugate products of complex correlations. As the simulation results showed, it allowed for joint estimation of the signal parameters (*i.e.*, the initial frequency and chirping rate) and data bits (bit sync and/ bit signs). There were ambiguous bit patterns and it could be easily resolved with an additional step of tests.

The block-integrating methods presented in this paper can handle large frequency changes caused by relative motion and clock drift. It can also remove data bits in an open-ended manner, allowing for new samples to be added on in the integration process as they become available. Indeed, when the BASIC algorithm of the present paper is applied in the downstream together with the MAGIC (i.e., the multiresolution adjustable grid interpolated correlator) [8] in the upstream, a new GPS receiver architecture emerges with open-loop acquisition and estimation. It is in contrast to the conventional receiver architecture that uses closed-open acquisition and tracking. This open-loop acquisition and estimation architecture is particularly suitable for software radio receivers with snapshot solutions. Research is under way to further advance this concept.

ACKNOWLEDGMENTS

Research supported in part under Contracts No. FA8650-05-C-1808 and FA8650-05-C-1828, which are gratefully acknowledged.

REFERENCES

[1] S. Barbarossa, "Analysis of Multicomponent LFM Signals by a Combined Wigner-Hough Transform," *IEEE Trans. on Signal Processing*, 43(6), June 1995.

[2] E.D. Kaplan and C.J. Hegarty (eds.), *Understanding GPS: Principles and Applications* (2nd Ed.) Artech House Publishers, Norwood, MA, 2006.

[3] P. Misra and P. Enge, *Global Positioning System, Signals, Measurements, and Performance*, Ganga-Jamuna Press, 2001.

[4] B.W. Parkinson and J.J. Spilker Jr. (eds.), *Global Positioning System: Theory and Applications*, AIAA, 1996.

[5] J.B.Y. Tsui, *Fundamentals of Global Positioning System Receivers - A Software Approach*, John Wiley & Sons, Inc., 2000.

[6] W.D. Wirth, *Radar Techniques Using Array Antennas*, IEE, London, UK, 2001.

[7] J.C. Wood and D.T. Barry, "Linear Signal Synthesis Using the Radon-Wigner Transform," *IEEE Trans. on Signal Processing*, 42, 1994.

[8] C. Yang, "GPS Signal Tracking with Kalman Filter Based on Joint Code Delay and Carrier Phase and Frequency Error Discriminator," *Proc. of ION-AM'04*, Dayton, OH, June 2004.

[9] C. Yang and E. Blasch, "A New Method for Extended Radar Pulse Integration Subject to Large Doppler Change," *Workshop on "Radar Resolution, Nonlinear Estimation, and Other Gratuitous Remarks on the Back of Envelope: A Tribute to Fred Daum*," Monterey, May 2007.

[10] C. Yang and S.W. Han, "Block Accumulating Coherent Integration Over Extended Interval (BACIX) for Weak GPS Signal Acquisition," *Proc. of ION-GNSS'06*, Ft. Worth, TX, September 2006.

[11] C. Yang, M. Miller, T. Nguyen, and E. Blasch, "Comparative Study of Coherent, Non-Coherent, and Semi-Coherent Integration Schemes for GNSS Receivers," *Proc. of ION-AM'07*, Boston, MA, April 2007.

[12] C. Yang, M. Miller, T. Nguyen, and E. Blasch, "Wigner-Hough/Radon Transform for GPS Post-Correlation Integration," *Proc. of ION-GNSS'07*, Fort Worth, TX, September 2007.